

**Imperial College
London**



Amin Nadimy

Applied Modelling and
Computational Group,
Department of Earth Science
and Engineering

Supervisors:
Professor C. C. Pain, Dr P. Salinas, Dr A. I.
Obeyesekara and Dr A. Nicolle (BP)

ICL-ICAM-BP

24th March 2021

Dynamic semi-structured meshes for fast numerical simulation of Multi-Phase Modelling in the energy industry

Starting date: 01 October 2020

Aim:

This project will develop and implement a semi-structured mesh within the Multi-Fluidity project to significantly improve its speed.

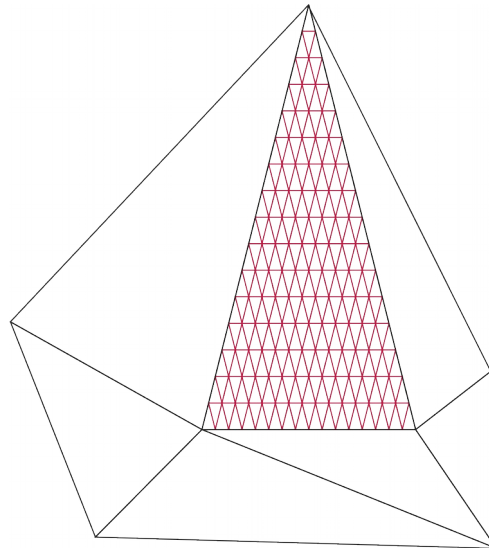


Figure 1. Semi-structured mesh.

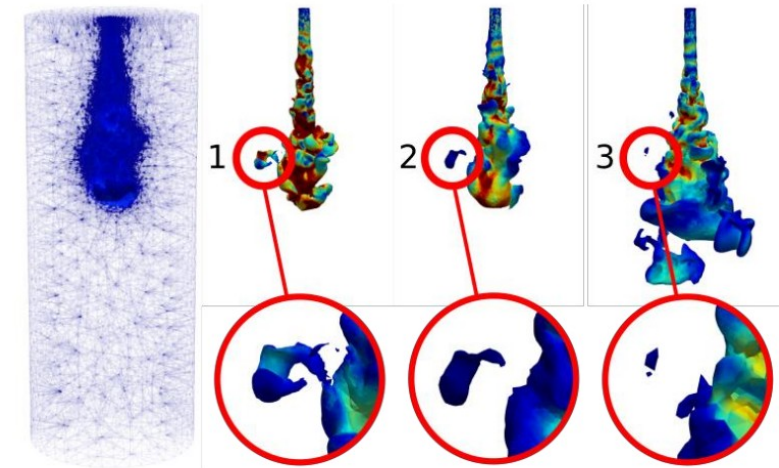


Figure 2. Creation and dispersion of a droplet.

Starting date: 01 October 2020

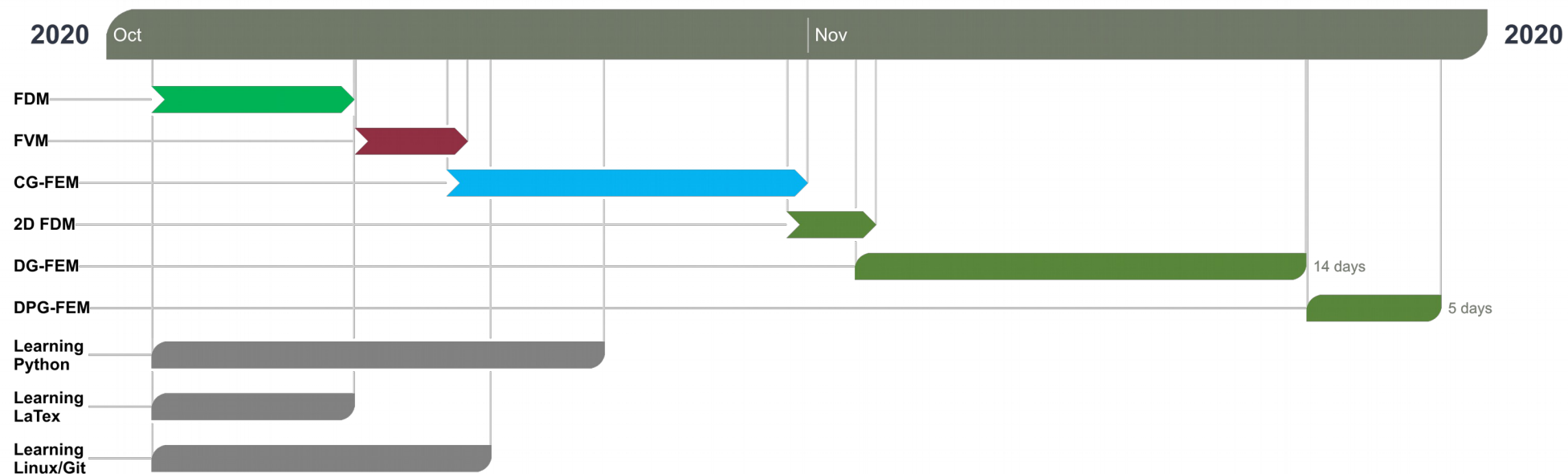


Figure 3. Work plan from October to mid-December 2020.

- 1D-DG Petrov-Galerkin FEM: 2 documents

1- Report

8.1.1.1 Diffusion Form

$$\int_{\Omega} \phi_i r d\Omega + \int_{\Omega} \nu \left(\frac{\partial U}{\partial t}, \frac{\partial U}{\partial x} \right)^T d\Omega = 0$$

where ν is the diffusion coefficient.

$$\underbrace{\sum_{j=1}^2 \frac{\partial U_j}{\partial t} \int_{\Omega} \phi_i \phi_j d\Omega - \sum_{j=1}^2 U_j \int_{\Omega} c \phi_j \frac{\partial \phi_i}{\partial x} d\Omega + \sum_{j=1}^2 U_j \oint_{\Gamma_e} \hat{n} \cdot c \phi_j \phi_i d\Gamma_e}_{\text{1st part}} + \underbrace{\sum_{j=1}^2 \frac{\partial U_j}{\partial t} \int_{\Omega} \nu \phi_j d\Omega + \sum_{j=1}^2 U_j \int_{\Omega} c \nu \frac{\partial \phi_j}{\partial x} d\Omega}_{\text{Stabilisation part}} = 0$$

$$\sum_{j=1}^2 \frac{\partial U_j}{\partial t} \left(\int_{\Omega} \phi_i \phi_j d\Omega + \int_{\Omega} \nu \phi_j d\Omega \right) + \sum_{j=1}^2 U_j \left(\int_{\Omega} c \nu \frac{\partial \phi_j}{\partial x} d\Omega - \int_{\Omega} c \phi_j \frac{\partial \phi_i}{\partial x} d\Omega \right) + \sum_{j=1}^2 U_j \oint_{\Gamma_e} \hat{n} \cdot c \phi_j \phi_i d\Gamma_e = 0$$

$$\nu = \frac{r P^* r}{\|\nabla_{xt} U\|^2}$$

$$P^* = \frac{1}{4} (||J_{xt}^{-1} c||_2)^{-1} = \frac{\Delta x}{8c}$$

where J_{xt} is space-time Jacobian matrix:

1- Theory

\mathbf{P}_{xt}^* is a function of \mathbf{A}_{xt}^* and the size and shape of the elements, for example:

$$\mathbf{P}_{xt}^* = \frac{1}{4} (||\mathbf{A}_{xt}^* \cdot \nabla_{xt} \mathbf{N}_{xti}||_2)^{-1}, \quad (37)$$

or using the 2 matrix norm and the space-time Jacobian matrix \mathbf{J}_{xt} :

$$\mathbf{P}_{xt}^* = \frac{1}{4} (||\mathbf{J}_{xt}^{-1} \mathbf{A}_{xt}^*||_2)^{-1}. \quad (38)$$

Since the matrices \mathbf{A}_t^* , \mathbf{A}_x^* , \mathbf{A}_y^* , \mathbf{A}_z^* that go to make up

$$\mathbf{A}_{xt}^* = (\mathbf{A}_t^{*T}, \mathbf{A}_x^{*T}, \mathbf{A}_y^{*T}, \mathbf{A}_z^{*T})^T \quad (39)$$

are diagonal the matrix \mathbf{P}_{xt}^* is also diagonal. In the traditional Petrov Galerkin method $\mathbf{A}_{xt}^* = \mathbf{A}_{xt}$ in the above and \mathbf{P}_{xt} replaces \mathbf{P}_{xt}^* . The finite element space-time Jacobian matrix for 3D time dependent problems is:

$$\mathbf{J}_{xt} = \begin{pmatrix} \mathbf{I} \frac{\partial t}{\partial t'} & \mathbf{I} \frac{\partial x}{\partial t'} & \mathbf{I} \frac{\partial y}{\partial t'} & \mathbf{I} \frac{\partial z}{\partial t'} \\ \mathbf{I} \frac{\partial t}{\partial x'} & \mathbf{I} \frac{\partial x}{\partial x'} & \mathbf{I} \frac{\partial y}{\partial x'} & \mathbf{I} \frac{\partial z}{\partial x'} \\ \mathbf{I} \frac{\partial t}{\partial y'} & \mathbf{I} \frac{\partial x}{\partial y'} & \mathbf{I} \frac{\partial y}{\partial y'} & \mathbf{I} \frac{\partial z}{\partial y'} \\ \mathbf{I} \frac{\partial t}{\partial z'} & \mathbf{I} \frac{\partial x}{\partial z'} & \mathbf{I} \frac{\partial y}{\partial z'} & \mathbf{I} \frac{\partial z}{\partial z'} \end{pmatrix}, \quad (40)$$

where the variables with t' are the local variables and where \mathbf{I} is the $\mathcal{M} \times \mathcal{M}$ identity matrix in which \mathcal{M} is the number solution variables at each DG node. For uniform space-time resolution with a time step size of Δt and an element size of Δx (in the x-direction), Δy (in the y-direction), Δz (in the z-direction), then:

$$\mathbf{J}_{xt} = \begin{pmatrix} \mathbf{I}_2^1 \Delta t & 0 & 0 & 0 \\ 0 & \mathbf{I}_2^1 \Delta x & 0 & 0 \\ 0 & 0 & \mathbf{I}_2^1 \Delta y & 0 \\ 0 & 0 & 0 & \mathbf{I}_2^1 \Delta z \end{pmatrix}. \quad (41)$$

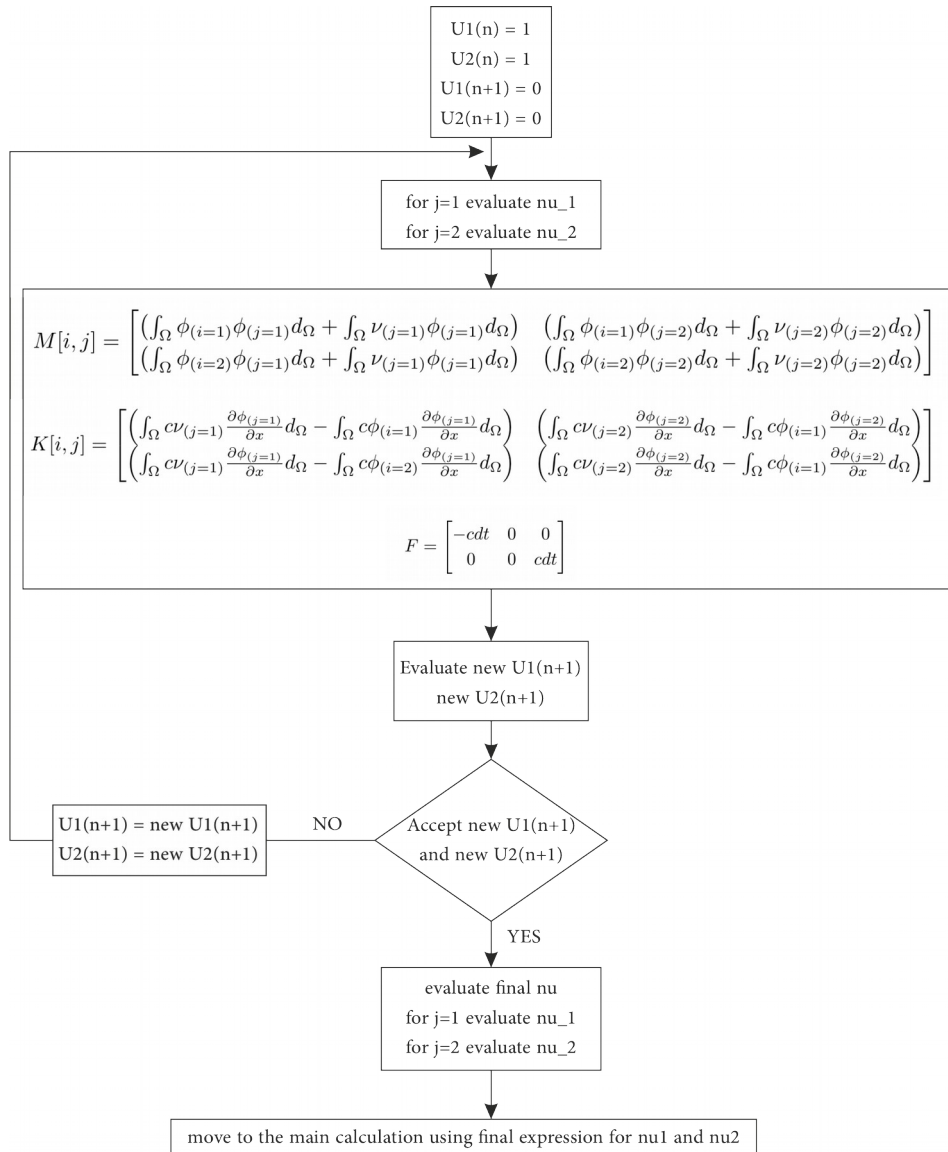


Figure 4. Flowchart for the DG Petrov-Galerkin diffusion method.

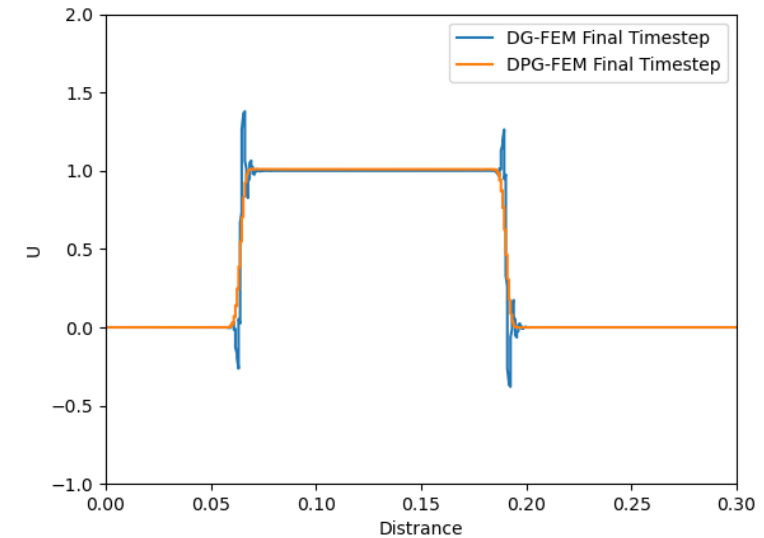


Figure 5. Illustration of the standard DG against DPG results for the same number of elements, 400.



- 2D FDM

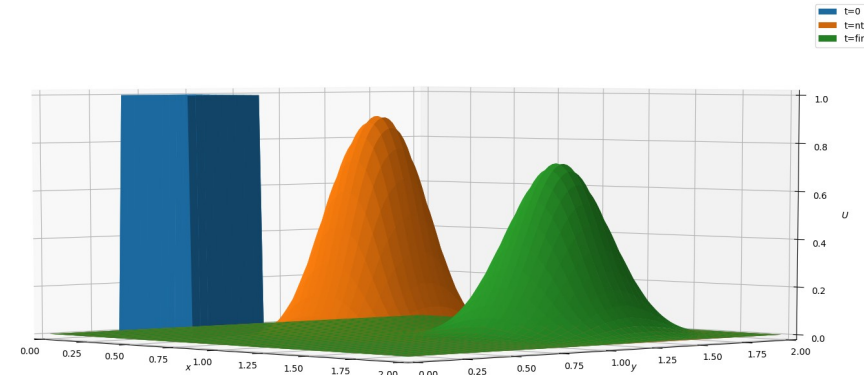


Figure 6. Travelling a square wave in 2D with 500 elements.

- 2D DG-FEM

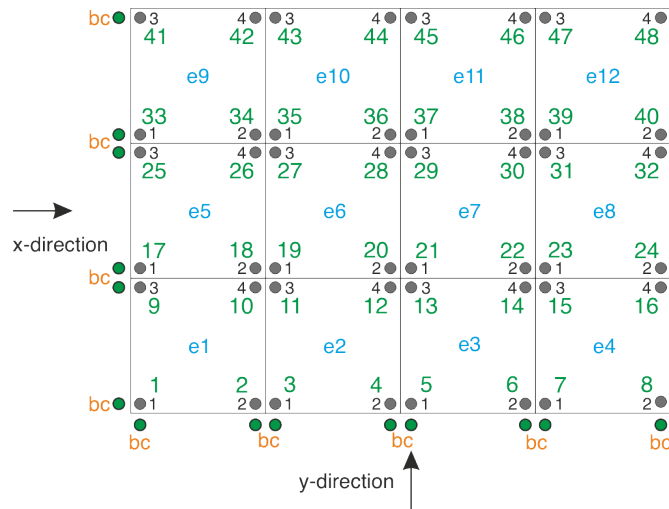


Figure 7. 2D domain with local & global node numbering.

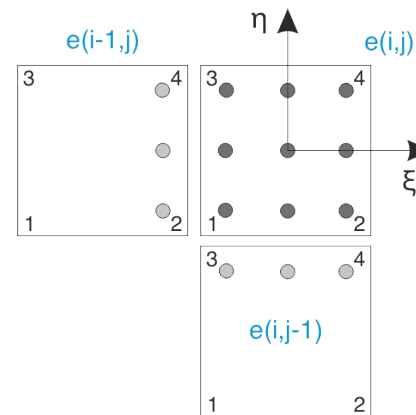


Figure 8. Volume integration using 3-point Gaussian quadrature method.

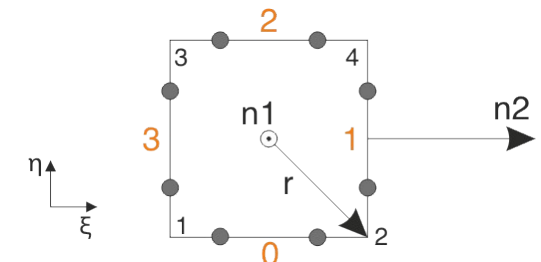


Figure 9. Surface integration using 2-point Gaussian quadrature method.

- Fortran Training

- IC-FERST Workshop

- Training sessions: multi-phase time-loop in the IC-FERST, identified the key subroutines corresponding to momentum, magma, porous media equations and their variables.
- Training for connecting & working with workstations, downloading and compiling IC-FERST code.
- 2D test files e.g. flow pass in a cylinder & collapsing water column. changed the flow velocity, the shapes and the positions of the problem.

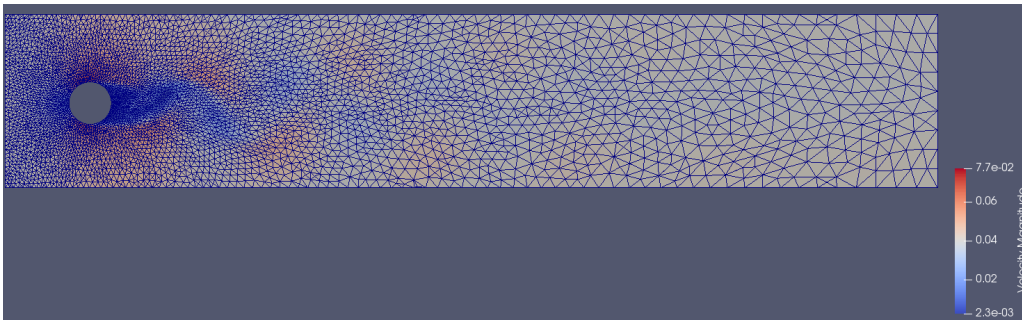


Figure 10. Flow pass a cylinder with the fixed mesh.

Simulation info:
Number of elements: 9444
Final time: 100
Time-step: 0.005
Reynolds number: 3900

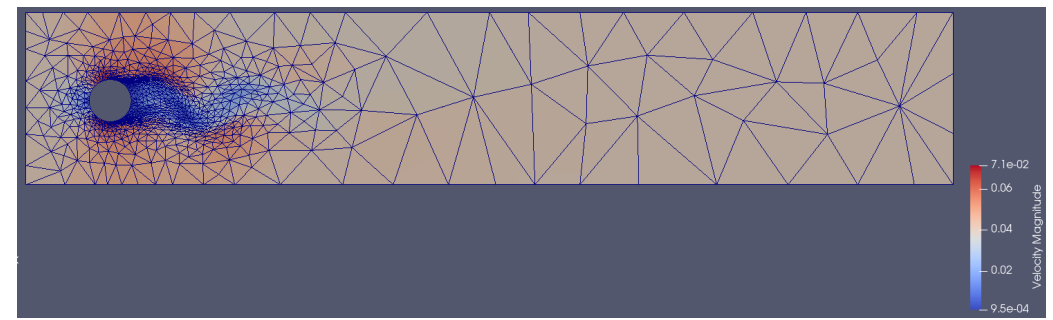


Figure 11. Flow pass a cylinder with the adaptive mesh.

Simulation info:
Initial number of elements: 168
Final number of elements: 2032
Final time: 100
Time-step: 0.005
Reynolds number: 3900

- Fortran Training

- IC-FERST training

- Training sessions: multi-phase time-loop in the IC-FERST, identified the key subroutines corresponding to momentum, magma, porous media equations and their variables.
- Training for connecting & working with workstations, downloading and compiling IC-FERST code.
- 2D test files e.g. flow pass in a cylinder & collapsing water column. changed the flow velocity, the shapes and the positions of the problem.

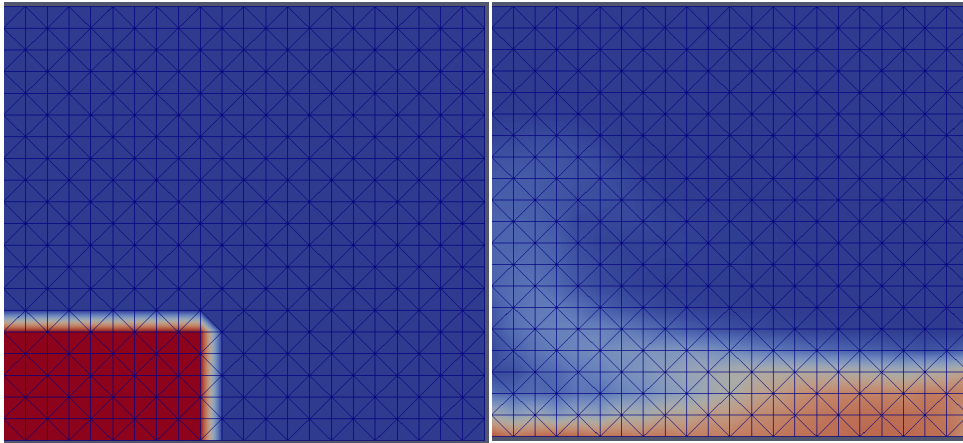


Figure 12. Collapsing water column under gravity with a fixed mesh.

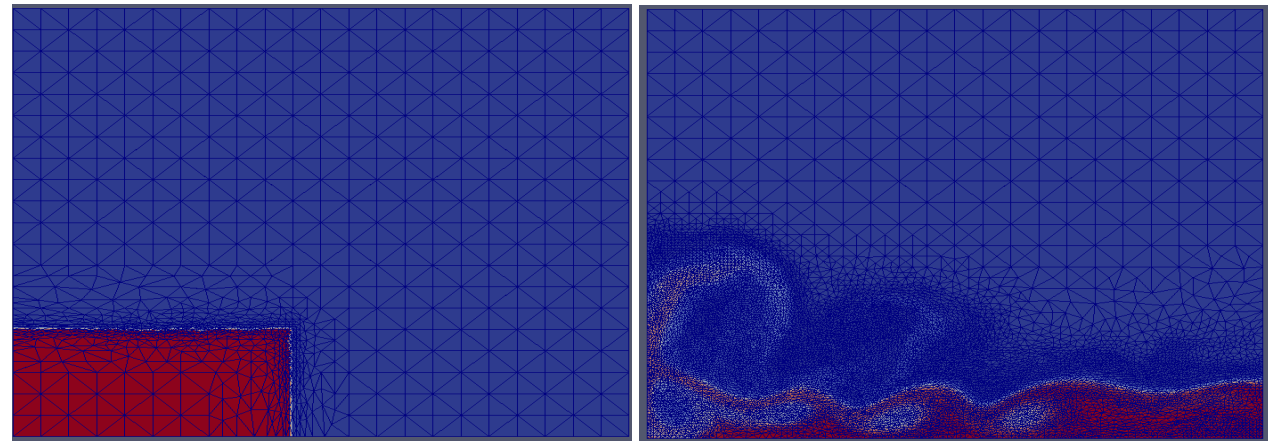


Figure 13. Collapsing water column under gravity with the adaptive mesh.

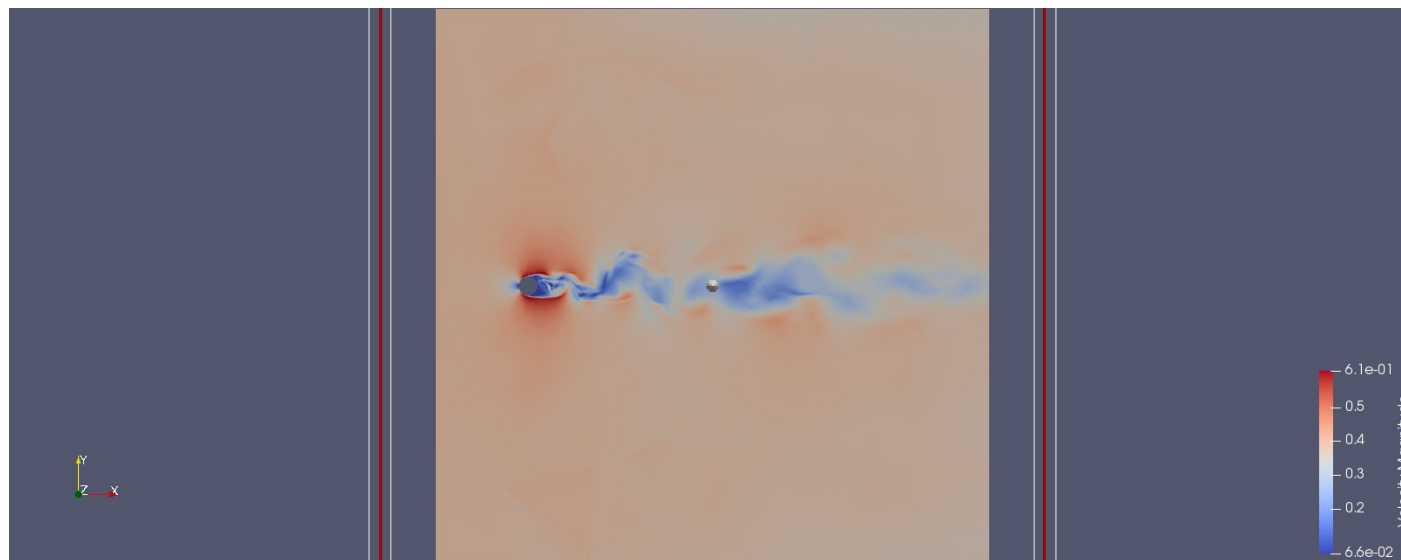


Figure 14. Flow pass in a cylinder in 3D with the adaptive mesh.

Simulation info:
Initial number of elements: 8470
Final number of elements: 21480
Final time: 0.76
Time-step: 0.005
Reynolds number: 3900

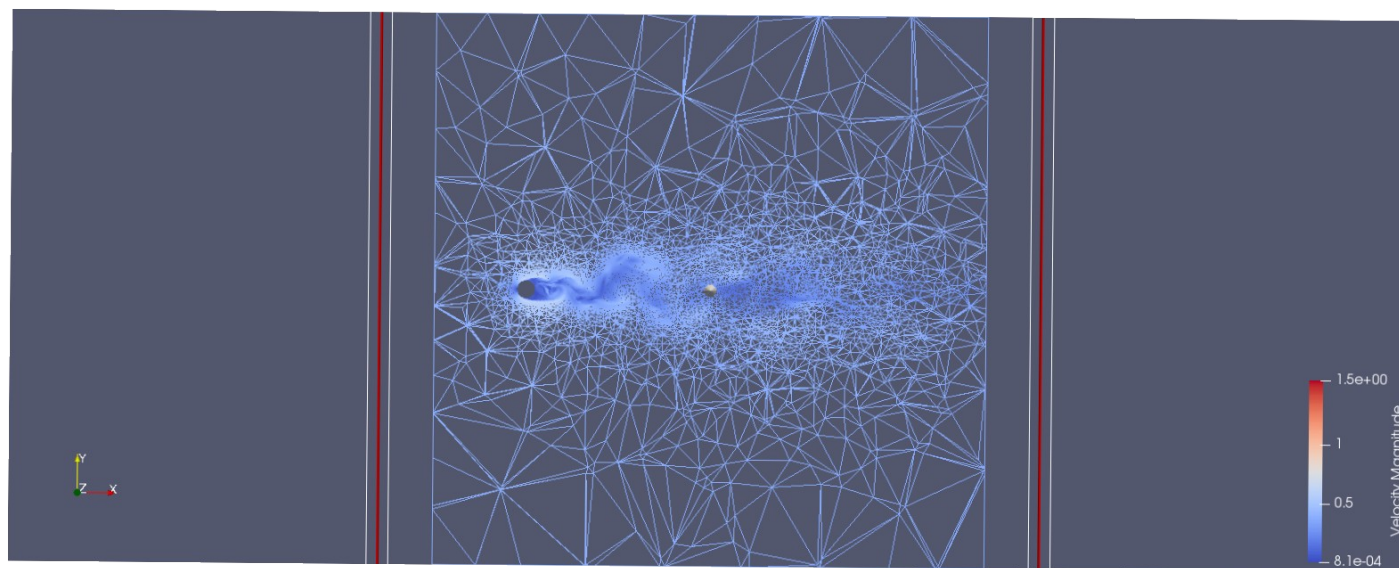


Figure 15. Sliced mesh view for the flow pass in a cylinder problem in 3D with the adaptive mesh.



Regular weekly meetings

- AMCG catch-up
- Porous media/Inertia
- BP catch-up

Theory

- Delaunay and barycenter triangulation (a few days)
- Voronoi diagram
- Structured mesh generation
- Unstructured mesh generation (~a month)
- Semi-structured mesh

Near-future work

- Will be working with Dr. Obeysekara on the mixing tank problem (end of March)
- 2D 1st order square wave DG-FEM (end of March)
- semi-structured 2D DG-FEM.
- Will be work with Prof. Pain and others on the Fortran code for semi-structured and with space-time within ICFERST/FLUIDITY.

END